Science of the Total Environment 859 (2023) 160105

Contents lists available at ScienceDirect

Science of the Total Environment

journal homepage: www.elsevier.com/locate/scitotenv

How will warming affect the growth and body size of the largest extant amphibian? More than the temperature–size rule

Wei Zhu, Tian Zhao, Chunlin Zhao, Cheng Li, Feng Xie, Jiongyu Liu, Jianping Jiang *

CAS Key Laboratory of Mountain Ecological Restoration and Bioresource Utilization & Ecological Restoration and Biodiversity Conservation Key Laboratory of Sichuan Province, Chengdu Institute of Biology, Chinese Academy of Sciences, Chengdu 610041, China

HIGHLIGHTS

- Warming likely reduces the body size of adult Chinese giant salamander.
- Diet rich in lipid may alleviate the influence of warming on their body size.
- Warming caused metabolic disorder resembling glycogen storage disease in this animal.
- Glycogen metabolism likely constrains their growth performance at higher temperature.
- Prey abundance and nutrient composition should be considered in their conservation.

GRAPHICAL ABSTRACT

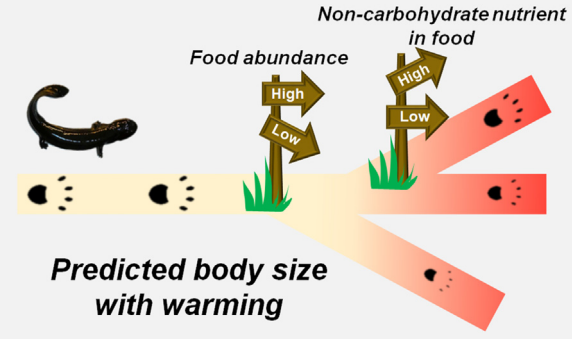

ARTICLE INFO

Editor: Sergi Sabater

Keywords:
Biological conservation
Chinese giant salamander
Metabolic switch
Organ heterogeneity
Transcriptomics
Warming

ABSTRACT

Declining body size is a universal ecological response to global warming in ectotherms. Ectotherms grow faster but mature at a smaller size at higher temperatures. This phenomenon is known as the temperature–size rule (TSR). However, we know little about the details of the relationship between temperature and size. Here, this issue was studied in the Chinese giant salamander (*Andrias davidianus*), one of the largest extant amphibians and a flagship species of conservation in China. Warm-acclimated *A. davidianus* larvae (25 °C) had accelerated development but little superiority in body growth when compared to their 15 °C counterparts when fed with red worm. This predicts a drastic decrease in adult body size with warming. However, a fish diet (more abundant lipid and protein) improved the growth performance at 25 °C. The underlying mechanism was studied. Warm-acclimated larvae had enlarged livers but shortened tails (fat depot). Their livers suffered from energy deficiencies and decreased protein levels, even when protein synthesis and energy metabolism were transcriptionally upregulated. This could be a direct explanation for their poor growth performance. Further analyses revealed a metabolic disorder resembling mammal glycogen storage disease in warm-acclimated larvae, indicating deficiency in glycogen catabolism. This speculation is consistent with their increased lipid and amino acid catabolism and explained the poor energy conditions of the warm-acclimated larvae. Additionally, a deficiency in glycogen metabolism explains the different efficiency of worm and fish diets in supporting the growth of warm-acclimated larvae, even when both diets were provided sufficiently. In conclusion, our results suggest that the relationship between temperature and body size can be flexible, which is a significant finding in terms of the TSR. The underlying metabolic and nutrient mechanisms were revealed. This knowledge can help deepen our understanding of the consequences of warming and can contribute to the conservation of *A. davidianus*.

* Corresponding author.
E-mail addresses: zhuwei@cib.ac.cn (W. Zhu), zhaotian@cib.ac.cn (T. Zhao), licheng@cib.ac.cn (C. Li), xiefeng@cib.ac.cn (F. Xie), liujy@cib.ac.cn (J. Liu), jiangjp@cib.ac.cn (J. Jiang).

http://dx.doi.org/10.1016/j.scitotenv.2022.160105
Received 8 July 2022; Received in revised form 2 November 2022; Accepted 6 November 2022
Available online 9 November 2022

1. Introduction

Climate change poses a great challenge to the health and productivity of ecosystems. The past century has seen a 1.1 °C rise in the global average temperature, and global warming of 2 °C will be exceeded unless extreme reductions in CO_2 and other greenhouse gas emissions occur in the coming decades (IPCC, 2021). Global warming may affect the distribution, phenology, and adaptation of animals (Hughes, 2000). Although animals may engage in behavioral thermoregulation (e.g., finding shelter and migration) to avoid adverse environmental temperatures (Ortega et al., 2016; Ye et al., 2021), they may still experience prolonged periods of time at suboptimum temperatures, especially those with limited migration capacity, e.g., the amphibians (Gunderson and Stillman, 2015; Kearney et al., 2009). Increasing evidence indicates that reduced body size is the third universal ecological response to global warming in animals (Baudron et al., 2014; Daufresne et al., 2009; Sheridan and Bickford, 2011). Body size is a fundamental biological trait that shapes many physiological and ecological properties (e.g., fecundity, population growth rate, competitive interactions) (Fryxell et al., 2020). For example, a change in size structure has top-down and bottom-up effects in ecosystems (Brose et al., 2012), and the loss of large predators will have great consequences on trophic control and the biomass structure in food webs (DeLong et al., 2015). The standard water loss rate through evaporation is negatively correlated with body mass in amphibians (Heatwole et al., 1969), and thus a reduction in body size is likely to make these desiccation-sensitive animals more vulnerable to extinction. Thus, revealing the mechanisms that link body size and environmental temperatures has great implications for biological conservation in the context of global climate change.

There are several explanations for the negative relationships between temperature and body size within non-extreme temperature scopes (temperatures allowing an organism to develop and reach maturity). When food is limited, the metabolic demands, which are exponentially increased with temperature (Gillooly et al., 2001), likely contribute to the reduced body size in ectotherms at higher temperatures (Sheridan and Bickford, 2011). This is because the energy must be divided between metabolic maintenance, growth, storage and reproduction (Heino and Kaitala, 2001; Zhu et al., 2021b), and the increased energy demands for cellular and metabolic homeostasis at higher temperatures likely limit the resource availability for somatic growth. Thus, increased food intake and shifted feeding behavior are proposed to be potential adaptive strategies to warming in ectotherms (Johansen et al., 2015). However, even when food is available, reduced body size at maturity is still observed in ectotherms at higher temperatures (Bizer, 1978; Fischer and Fiedler, 2002; Ghosh et al., 2013). This phenomenon has been dubbed the temperature–size rule (TSR) (Atkinson, 1994). The TSR states that higher temperatures increase the growth rate (increase in somatic mass) and development rate (differentiation from egg to adult) simultaneously, while decreasing the adult body size (Ohlberger, 2013). This is because temperature can affect development independently of growth (Davidowitz and Nijhout, 2004; Kuparinen et al., 2011), and development has stronger temperature dependence than growth (Forster et al., 2011). Although the TSR describes the general variation trend of body size with an increase in of temperature, our limited understanding of the molecular mechanisms involved makes it difficult to assess the degree and flexibility of body size reduction at higher temperatures. Thus, there is an urgent need for knowledge on the mechanistic links between the temperature and growth rate, which will greatly improve our ability to predict the responses of species to future climate warming (Gardner et al., 2011).

Given that the thermal properties of some organ systems or cellular processes can constitute the initial limitation for the thermal performance of the whole organism (Eliason Erika et al., 2011; Lemieux et al., 2010), it is essential to reveal the critical organs or cellular processes that may constrain growth at non-extreme temperatures in order to understand the relationship between body size and temperature. One of the best known hypotheses is that the cardiovascular capacity can't keep up with the increase in oxygen requirements caused by an increase in temperature (Pörtner, 2002; Pörtner and Farrell, 2008). This means that decreased aerobic scope at higher temperatures may be a physiological cause for the reduced growth rate, as a bigger body size may cause greater restrictions in terms of oxygen availability (Atkinson et al., 2006; Forster et al., 2012). However, whether the aerobic scope is a single unifying principle that explains the thermal limitation of physiological performance is still controversial (Claëssson et al., 2016; Grans et al., 2014; Lefevre, 2016). It is possible that the molecular processes shaping the thermal responsiveness of somatic growth may vary with species due to their different evolutionary trajectories. Revealing these biological processes will not only lead us to a mechanistic understanding of the relationship between body size and temperature but may also provide us with some clues as to how to manipulate the response of a species to temperature changes, which has great significance for species conservation.

The Chinese giant salamander (*Andrias davidianus*) is one of the largest extant amphibian species and has been crowned as a living fossil (Gao and Shubin, 2003). This species was once widely distributed in central and southern China (Fei et al., 2006; Wang et al., 2017), but its wild populations have declined dramatically due to habitat degradation, pollution, and overexploitation in recent decades (Jiang et al., 2021; Zhao et al., 2020). The Chinese giant salamander has been evaluated as Critically Endangered (IUCN, 2016), and it is now a flagship species for biological conservation in China (Jiang et al., 2016; Zhao et al., 2022). According to laboratorial studies, *A. davidianus* larvae are sensitive to temperature variations (Hu et al., 2019; Zhang et al., 2014; Zhu et al., 2021a). Their empirical optimal temperature for growth is 15–21 °C (Chen et al., 1999; Hu et al., 2019). When the water temperature is higher than 25–28 °C or lower than 7 °C, their feeding behavior changes and their growth rate begins to decline (Hu et al., 2019; Mu et al., 2011; Wang, 2004). The thermal regimes of wild *A. davidianus* are seasonally variable. For example, the monthly mean temperature of a natural *A. davidianus* habitat in Henan province varies from 1.5 °C in January to 25–26 °C in July (Ge and Zheng, 1994; Wang et al., 2002). Field observations suggest that the occurrence of *A. davidianus* negatively correlates with temperature within the range of 19–25 °C (unpublished data). These results suggest that *A. davidianus* prefer cooler temperatures. However, future global warming will likely increase the amount of time they spend at higher temperatures, which potentially constitutes a challenge to their long-term survival and fitness in the wild (Zhang et al., 2020; Zhao et al., 2020). Moreover, given that Chinese giant salamanders are top predators in their habitats, the climatic influence on their survival and body size are likely to have a top-down cascading effect on the prey density in natural communities (Rudolf, 2012). Thus, studying the influence of warming on these animals has great significance for ecological and biological conservation.

In this study, the growth traits were tracked and compared for *A. davidianus* larvae raised at the empirical optimum temperature (15 °C) and a temperature near the maximum values in their natural habitats (25 °C, sub-optimum) (Ge and Zheng, 1994). Although both temperatures are within the thermal scope of their wild habitats, warming will likely change the relative proportion of exposure time to these two temperatures. Multi-organ transcriptomics and metabolomics, along with physiological and biochemical analyses, were conducted to reveal the organ systems and cellular processes that may limit the thermal performance of *A. davidianus* larvae. Our main were to reveal the following (1) The influence of warming on the growth rate and body traits of *A. davidianus* larvae. We speculated that warming would unequally affect the developmental and growth rates in these animals. (2) The molecular mechanisms underlying the relationship between the temperature and growth traits of *A. davidianus* larvae. Given that this animal exhibits remarkable heterogeneity in response to cold at both the organ and molecular levels (Zhu et al., 2022b), we hypothesized that the thermal adaptability of *A. davidianus* larvae would be constrained by some critical molecular processes. (3) Whether the influence of temperature on body size is plastic. Since food composition can shape the thermal tolerance limits of *A. davidianus* larvae (Zhao et al., 2022), we speculated that nutrients may also be a critical factor in determining their growth performance at higher temperatures. The results are expected to deepen our understanding of the fate of this important species in the future.

More importantly, they may extend our knowledge of thermal physiology theories and provide some new insights into biological conservation.

2. Methods and materials

2.1. Animals

The farm (102°10′05″ E, 29°52′36″ N) for *A. davidianus* artificial culture is located in Hongya County, Sichuan province in China, where the larvae were maintained at 15 ± 1.14 °C (water temperature). These animals yearly breed in August and September, and their eggs hatch in August, September, and October. The larvae grow for 3–5 years to reach their sexual maturity. We studied the morphological development of *A. davidianus* embryos and larvae in 2018–2020. The early development stages, from fertilized egg to the formation of fifth digit in hindlimb, lasts approximate 70 days in the artificial farm (Fan et al., 2022). After this period, there were no longer typical morphological traits to finely distinguish the change in developmental stages, but the body mass and length of the larvae were still recorded aperiodically (with an interval of dozens of days, e.g., 172, 243, 277, and 342 days after hatching, d.a.h). For each timepoint, several individuals (n = 3–7) were sacrificed after being euthanized in a 0.1 % w/v MS-222 solution and dissected to measure the relative size of some typical organs (e.g., liver) (Supplementary data 1). All protocols in this study were reviewed and approved by the Animal Ethical and Welfare Committee of Chengdu Institute of Biology, Chinese Academy of Science, China. (permit: CIB20160305 and 20,191,105), in compliance with the ARRIVE guidelines 2.0 (Percie du Sert et al., 2020) and Guide for the Care and Use of Laboratory Animals (8th edition) published by National Research Council (US) Committee for the Update of the Guide for the Care and Use of Laboratory Animals (2011).

2.2. Laboratorial culture and thermal acclimation

Larvae of the giant salamander were collected from the artificial farm mentioned above. In the laboratory, these larvae were fed daily with red worms (larvae of *Chironomus* sp.). The photoperiod was maintained at 12 L:12D. Independent thermal acclimation experiments were conducted in 2018, 2019, and 2020. The larvae were randomly divided into two thermal groups and acclimated at 15 ± 0.5 °C (control group, empirical optimum) or 25 ± 0.5 °C (warm group, upper thermal limit allowing for robust growth and near to the maximum temperature of their natural habitats).

For the acclimation in 2018, *A. davidianus* larvae hatched from a single clutch were collected at approximately the 100th d.a.h (n = 35 and 33 for control and warm group, respectively). For each thermal group, the larvae were placed into two plastic containers (42 × 30 × 10 cm, water depth = 5 cm; 16–18 individuals per container). The acclimation lasted for 330 days. The larvae were fed daily with sufficient commercial red worms for the first 260 days, then the diet was replaced with fish fry for the subsequent 70 days. The water was replaced daily before feeding. It should be mentioned that the red worm is empirically recommended as an optimum diet for the larvae at the first age, as it is better for larvae growth than other diets (e.g., fish fry and chicks) in farms (approximate 15 °C). The variations in BM and TOL were recorded (Supplementary data 1), and the body condition was estimated with the scaled mass index. At the 80th day after acclimation, 15 larvae from each group were euthanized by immersion in a 0.1 % w/v MS-222 solution (2000 mL) at their respective temperature for >10 min (Zhu et al., 2022a) and then decapitated for dissection. The tissue samples were weighed and collected for transcriptomics, metabolomics, and biochemical analyses.

For the acclimation in 2019, *A. davidianus* larvae hatched from a single clutch were collected at approximately the 140th d.a.h. Each thermal group included 60 individuals, which were equally divided into three plastic containers (29 × 20 × 9.7 cm, with 3.5 L tap water) as three parallel replicates (20 individuals per container). The larvae were fed with sufficient commercial red worms daily throughout the treatment. The water was replaced daily before feeding. The acclimation lasted for 128 days. Their body mass (BM, g), total length (TOL, cm), tail length (from the cloaca to the tail-tips; cm), and snout–vent length (SVL, cm) were recorded 5, 26, 33, 41, 48, 55, 63, 70, 76, and 95 days after acclimation. The relative tail length was calculated as the ratio of tail length to SVL or TOL. The body condition was estimated using the scaled mass index with the equation $sM_i = M_i \times \left(\frac{L_{mean}}{L_i}\right)^{b_{sma}}$ (Peig and Green, 2009), where M_i and L_i are the BM and TOL of individual i, respectively; b_{SMA} is the scaling exponent estimated by the standardized major axis (SMA) regression on ln-transformed BM and TOL (calculated using the smatr package in R) (Warton et al., 2012); L_{mean} is the arithmetic mean value of TOL; and sM_i is the predicted BM for individual i when the L_i is standardized to L_{mean}. The absolute growth rate (g/d) was defined as daily average increment in total BM of the larvae from the same container. The daily food intake (g/d) was recorded every few days (see the detailed timepoints in Supplementary data 1). Food intake was defined as the total amount of food consumed by all individuals in a given container, and it was measured by calculating the difference between the initial and remnant food mass (wet mass) of a given day. The food conversion rate was calculated as the ratio of growth rate (g/d) to daily food intake (g/d).

For the acclimation in 2020, 150 larvae (hatching from a single clutch) were collected from the farm at their 120th d.a.h. These larvae were divided into five groups (n = 30 per group) to examine the influences of acclimation temperatures and diet types on their thermal limits (Zhao et al., 2022). Among them, there were two worm-fed groups acclimated to 15 and 25 °C, respectively. For these two groups, larvae were fed with sufficient commercial red worms daily throughout the treatment, and the water was replaced daily before feeding. These larvae were continued to be acclimated at their respective temperature after being measured for thermal limits at the 30th day of acclimation. After being acclimated for 160 days, ten larvae of each group were euthanized by immersion in a 0.1 % w/v MS-222 solution and sacrificed to measure body mass, total length, and organ mass (Supplementary data 1).

2.3. Transcriptional analyses

The larvae were collected on the 80th day after acclimation (2018). After being weighed and euthanatized using MS-222 (described above), the larvae were dissected to collect the brain, heart, liver, gill, forelimb, dorsal skin, and tail (1 cm from the cloaca site). The brain, heart, liver, gill, and fore limb were weighed to study the developmental allometry between groups. Then, these tissue samples were stored at −80 °C. The high-depth transcriptomes (>20 g for each sample) of single tissues were obtained using the second-generation sequence technology (n = 3 per tissue per group). In detail, the total RNA of each sample was extracted and purified using TRIzol (Invitrogen, Carlsbad, CA, USA) following the manufacturer's instructions. After being purified with poly-T oligo-attached magnetic beads, the mRNAs were fragmented. First-strand cDNA was synthesized using random hexamer primers. Second-strand cDNA synthesis was subsequently performed using DNA Polymerase I and RNase H. The remaining overhangs were converted into blunt ends via exonuclease/polymerase activities. After adenylation of the 3′ ends of the DNA fragments, adaptors were ligated to the products. Then, PCR was performed with a HIFI DNA polymerase, universal PCR primers, and Index (X) primer. The library preparations were sequenced on an Illumina HiSeq 2500 platform (PE150 strategy) from Annoroad (Beijing). For each sample, >20 g sequence data were obtained. The reads were queried against our whole length transcriptome (reference genome) (Zhu et al., 2022b) with RSEM and Bowtie2 (see the gene expression table in Supplementary data 2). The data of the control group were published in our previous study concerning the cold adaptation of *A. davidianus* (Zhu et al., 2022b). Differently expressed genes (DEGs) were identified by Student *t*-test and Benjamini and Hochberg's correction at a threshold of $p < 0.05$, or $q < 0.05$. Functional enrichment analyses were conducted by querying DEGs against the KEGG database (based on KOBAS 3.0, with default parameters).

2.4. Untargeted metabolomics

The liver, heart, brain, forelimb, and tail (n = 6 per tissue) of acclimated larvae (on the 80th day after acclimation) were measured for metabolic profiles. For each sample, 100 mg tissue powder was grinded in liquid nitrogen and extracted with 1 mL methanol: acetonitrile: water = 2:2:1 (v/v) (ultrasonication for 30 min × 2 and incubation at −20 °C for 1 h). After centrifugation at 12,000*g* for 15 min (4 °C), the supernatants were transferred into new tubes and freeze-dried. Samples were dissolved in 100 μL acetonitrile:water 1:1 (v/v) and analyzed by LC (1290 Infinity LC, Agilent) coupled with quadrupole-time-of-flight mass spectrometry (Triple TOF 5600+, AB SCIEX). The C18 HILIC column (ACQUITY UPLC HSS T3 1.8 μm, 2.1 mm × 100 mm, Waters) was equilibrated with 95 % (v/v) solvent A (25 mM ammonium acetate and 25 mM ammonium hydroxide in water). Separation was performed with 40–95 % solvent B (acetonitrile) at 0.3 mL/min as follows: 0–0.5 min, 95 % B; 0.5–7 min, decreasing B from 95 % to 65 %; 7–8 min, decreasing B from 65 % to 40 %; 8–9 min, 40 % B; 9–9.1 min, increasing B from 40 % to 95 %; 9.1–12 min, 95 % B. Metabolite data were obtained in both positive and negative ion modes with the following settings: ion source gas 1, 60; ion source gas 2, 60; curtain gas: 30; source temperature: 600 °C; ion spray voltage floating, ±5500 V; TOF MS scan *m/z* range: 60–1200 Da; product ion scan *m/z* range: 25–1200 Da; TOF MS scan accumulation time, 0.15 s/spectrum; product ion scan accumulation time, 0.03 s/spectrum. The MS/MS spectra were acquired by information-dependent acquisition with high sensitivity as follows: declustering potential, ± 60 V; collision energy, 30 eV. The data of control group were published in our previous study concerning the cold adaptation of *A. davidianus* (Zhu et al., 2022b). The data were processed using XCMS (http://metlin.scripps.edu/download/). The metabolites were identified by querying a standard library with an MS/MS spectrum. The relative abundances/concentrations of metabolites are presented as the ion intensities of their molecular ion peaks (see the metabolite abundance table in Supplementary data 3). Differently expressed metabolites were screened by Student's *t*-test and Benjamini and Hochberg's (BH) correction at a threshold of $p < 0.05$, or $q < 0.05$.

2.5. Biochemical analyses

The larvae (n = 10 per group) were collected on the 160th day after acclimation. After being weighed and euthanatized via the method described above, the larvae were dissected to collect the brain, liver, and heart. After adding 500 μL 0.1 M PBS (pH 7.4), approximately 50 mg of tissues was homogenized by a tissue grinder, followed by centrifugation at 1000*g* for 15 min (4 °C). The supernatant was ready for triglyceride and soluble protein determination. The remaining supernatant (300 μL) was mixed with 600 μL of 10 % trichloroacetic acid (TCA, w/v). After centrifugation at 1000*g* for 15 min, 300 μL of supernatant was transferred into a new tube containing 1200 μL of 95 % ethanol and allowed to rest overnight. After centrifugation at 1000*g* for 15 min, the precipitate was dissolved in 50 μL of water to form a glycogen solution.

2.5.1. Tissue protein level

The protein content in the liver, brain, and heart (n = 10 per tissue per group) was measured using a BCA protein assay kit (Solarbio Life Science, China). For each sample, 20 μL of supernatant was added to 200 μL BCA working solution and incubated at 37 °C for 30 min. The optical density of the mixtures at 562 nm was determined. The standard curve was constructed with a gradient dilution of 5 mg/mL BSA.

2.5.2. Tissue triglyceride level

The GPO-PAP method was used for the determination of the triglyceride level in the liver and blood (n = 10 per tissues per group). The triglyceride assay kit was purchased from Nanjing Jiancheng Bioengineering Institute, China. The reaction system included 2.5 μL of supernatant and 250 μL of reagent mixture (Tris-HCl, 100 mM; lipase ≥3000 U/L; ATP, 0.5 mM; glycerol kinase, ≥1000 U/L; glycerol 3-phosphate oxidase, ≥5000 U/L; peroxidase, ≥1000 U/L; 4-aminoprotepyrine, 1.4 mM; p-chlorophenol, 3 mM). After incubation at 37 °C for 10 min, the optical density at 510 nm of the mixtures was determined. A glycerol solution (2.26 mM) was used to generate a standard curve.

2.5.3. Tissue glycogen level

The liver glycogen was measured by anthrone (n = 10 per group). The reaction system of glycogen measurement included 5 μL of glycogen solution, 85 μL of water and 400 μL of 0.2 % anthrone in 80 % sulfuric acid. After incubation at 95 °C for 15 min and cooling at room temperature, the optical density of the mixtures at 626 nm was determined. Soluble starch (2 mg/mL) was used to generate a standard curve.

2.5.4. Identification of adipose tissue

Euthanatized larvae (n = 3) had their abdomens dissected and immersed in 500-fold water diluted 10 % (w/v) dithizone-ethanol solution (with 2 % (v/v) ammonia for solubilization) for >30 min. Tissues rich in fat would be stained with a dark green color, while other tissues were stained with an orange to red color (Zhu et al., 2019).

2.6. Statistical analyses

Statistical analyses were conducted on SPSS v25.0 (SPSS Inc., Chicago, USA). Kolmogorov–Smirnov and Shapiro–Wilk tests were conducted to check the deviation of the data from normal distribution. As larvae from the same container were repeatedly measured and they could not be distinguished from each other, the influence of temperature on body traits (i.e., weight, length, body condition, and relative tail length) and food intake were analyzed using a linear mixed model (LMM). To fit LMMs, the values of body traits at each timepoint were taken as the averages of the individuals from the same plastic container to avoid pseudo-replicates. We are interested in the variations of body traits with time, as well as the potential interactive effects between temperature and time, and thus we treat the time as a fixed factor in LMM. The LMM was built and optimized according to the information criteria (e.g., AIC and BIC values), e.g., whether the interactions between temperature and time kept in the final models. However, the use of average values in the LMM results in a significant loss of the degree of freedom, and thus we can't fully use the individual replications. Thus, the Mann–Whitney *U* test was also used to examine the intergroup differences at the individual level, but only for data collected at some crucial points (e.g., at the end of acclimation or diet shift). For the growth data collected at 2018, the number of parallels (n = 2) does not reach the lowest requirement for LMM (normal distribution of the data), and thus only Mann-Whitney *U* test was also conducted to examine the intergroups differences at individual level. The diffslope function (simba package in R) (Jurasinski and Retzer, 2012) and piecewise linear regression were used to examine the influence of diet shift on the growth performance of larvae at their respective temperature. The piecewise linear regressions were conducted on 1stOpt software (7D-Soft High Technology Inc., China). The differences in organ mass between groups were analyzed with ANCOVA, with BM as a covariate. The biochemical indexes were analyzed with Mann–Whitney *U* test or Kruskal–Wallis test. The graphs were generated by GraphPad Prism 5 or ggplot2 in R (Wickham, 2009).

3. Results

3.1. Growth at higher temperature

For acclimation in 2019 (Fig. 1a), the warm-acclimated group showed a higher growth rate of body mass ($p < 0.01$ for the interactive effect), but a significant difference ($p < 0.05$, simple effect analysis and Mann–Whitney *U* test) in BM was observed until the 95th day after acclimation (Fig. 1b). There was no difference in TOL between the groups ($p > 0.05$ for the temperature and interactive effects; Fig. 1c). The warm-acclimated larvae had a higher body condition score after 33 days of acclimation ($p < 0.05$, simple effect analysis; Fig. 1d). The warm group consumed much more food than

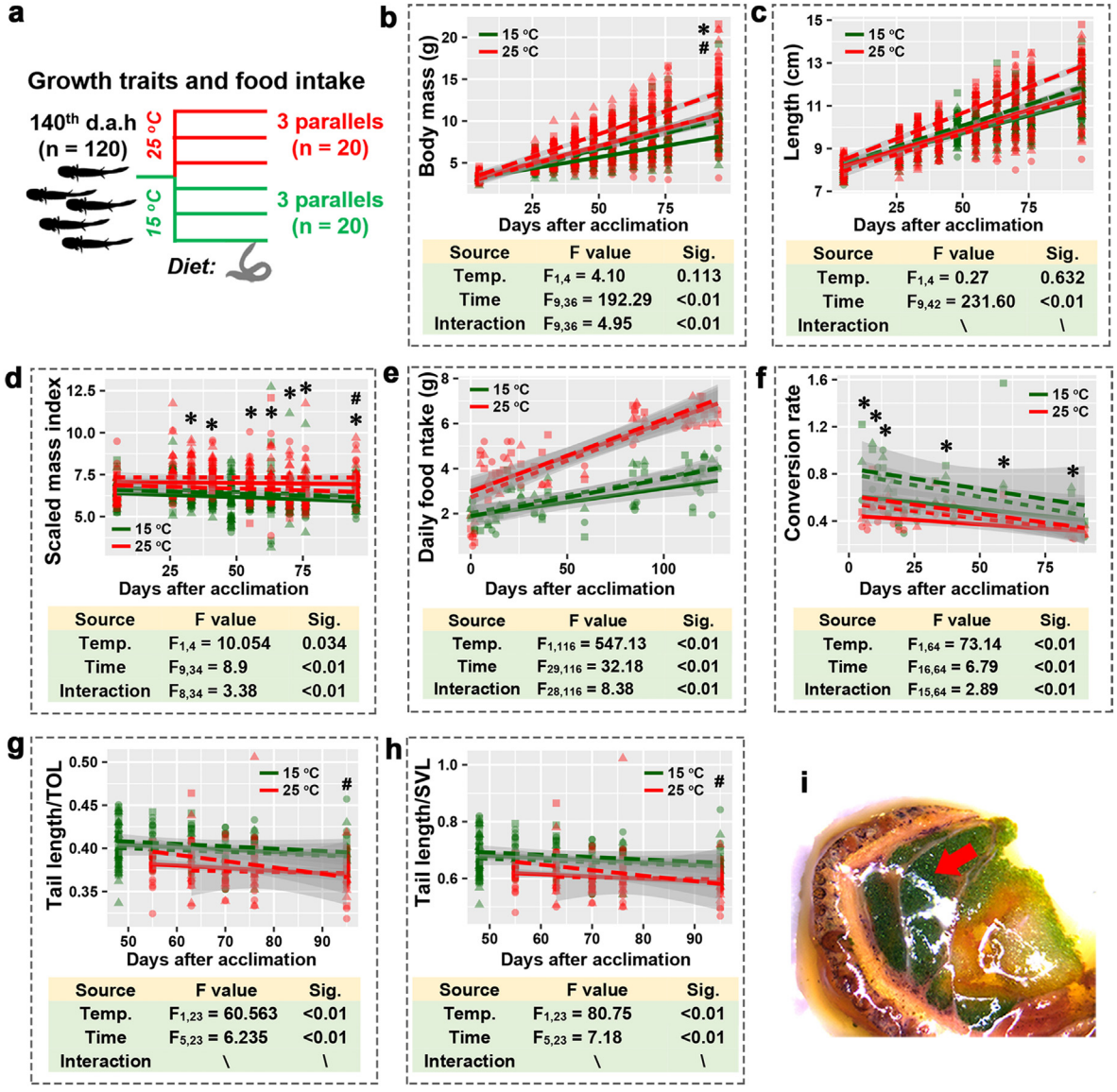

Fig. 1. Influences of temperature on body traits of *A. davidianus*. (a) Experimental design. (b) Influence of warming on growth of body mass (BM) (b), total body length (TOL) (c), and body condition (d). (e–f) Difference in daily food intake (e) and food conversion rate (f) between thermal groups. (g–h) Influence of warming on the ratio of tail length to TOL (g) and SVL (h) of *A. davidianus* larvae. The dots denote the values of each individual (for panel b–d and g–h) or parallel/container (for panel e–f) at the corresponding timepoint, while the lines denote the linear fitting of the values from the same parallel/containers, with the 95 % confidence interval being presented in gray. The colors of the lines and dots denote the thermal groups (red, warming group; green, control group), while the dot shapes and line types are used to distinguish values from different parallel/containers. The tables below present the results of the LMM. If there is a significant interactive effect between temperature and time, simple effects analysis is conducted to examine the intergroup difference for each timepoint. In this case, asterisks are used to denote significant intergroup difference at the corresponding timepoints. Note that the asterisks are not applied to denote the results of simple effect analysis on daily food intake (panel e), because the timepoints of food intake data are too dense to make a clear labeling. Simple effect analyses indicate significant differences in food intake at day 2, as well as all the timepoints after five days of acclimation. A '#' denotes significant intergroup difference ($p < 0.05$) at the corresponding timepoints examined by Mann–Whitney *U* test. (i) A photograph presenting the distribution of fat in the tail tissue (cross section). The tail is stained with anthrone, which highlights the tissue rich in fat with a dark green color. The red arrow denotes the fat tissue in the tail.

the control group (Fig. 1e), but its food conversion rate was lower ($p < 0.05$, simple effect analysis; Fig. 1f). The relative tail length decreased in warm-acclimated larvae ($p < 0.01$ for the temperature, LMM and Mann–Whitney U test; Fig. 1g–h), and this organ is the primary fat depot (Fig. 1i).

For the experiment conducted in 2018 (Fig. 2a), the red worm diet was replaced with a fish diet on the 260th day after acclimation, which had 2.62-fold higher lipid, 1.26-fold higher protein, and 10-fold lower carbohydrate content than the worm diet per unit mass (Fig. 2b). Similar results were obtained when the larvae were fed red worm. Significant intergroup differences were observed for neither BM nor TOL even after 257 days of acclimation ($p > 0.05$, Mann–Whitney *U* test; Fig. 2c–d). A higher body condition scores was again observed in warm group ($p < 0.01$; Fig. 2e). After the diet shift, the warm group showed accelerated growth in BM and TOL ($p < 0.01$, differences in the slopes), as is shown by an inflection in the relationship between time and body index (piecewise linear regression, Fig. 2f). The control larvae showed no significant changes ($p > 0.05$ for the differences in slopes) in growth of BM after diet shift, and their growth in TOL was even decreased ($p < 0.01$ for the differences in slopes). Additionally, significant differences in BM and TOL were observed after 9 and 24 days, respectively (simple effect analysis and Mann–Whitney *U* test; Fig. 2c–d). These results suggest that the relationship between body size and temperature was affected by factors other than food abundance.

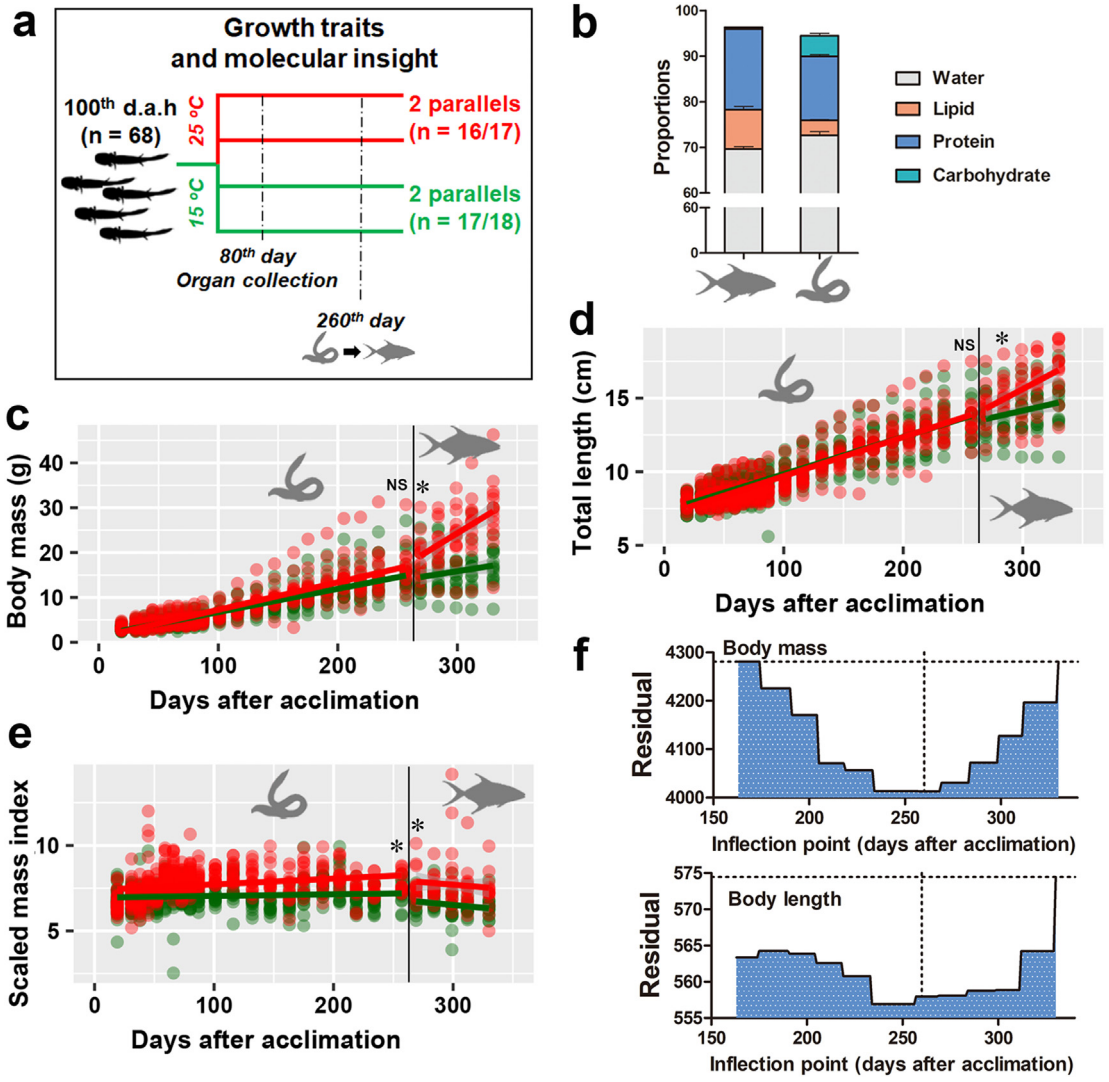

Fig. 2. Plasticity in the relationship between growth performance and temperature (2018). (a) Experimental design. (b) Nutrient composition of red worm and fish fry diet. (c–e) Influences of diet on the growth performance at higher temperature. The dots denote the values of each individual at the corresponding timepoint, while the lines denote the linear fitting of the values from the same parallel/containers, with the 95 % confidence interval presented in gray. The colors of the lines and dots denote the thermal groups (red, warming group; green, control group). The asterisks denote significant intergroup differences ($p < 0.05$) at the corresponding timepoints examined by Mann–Whitney U test. (f). Curve-fitting of the relationship between time and growth performance of larvae at 25 °C. Both normal and piecewise linear regressions were conducted on 1stOpt software. The vertical axis is the residual of the regression model, and the horizontal axis is the inflection point (days after acclimation) for the piecewise linear regression. The vertical and horizontal dashed lines denote the time of diet shift and the residual of normal linear regression. The results show that piecewise linear regression performs better than normal linear regression, and the best outcome is obtained when the inflection points are located at the time of the diet shift, which supports a change in the growth rate of the warm group after the diet shift.

3.2. Organ heterogeneity in response to warm acclimation

The warm-acclimated group had smaller gills and better developed forelimb than the control group at the 80th day after acclimation (180 d.a.h) (Fig. 3a), despite their BM being comparable (Fig. S1). The gills of the warm-acclimated group disappeared completely after 300 days of acclimation (400 d.a.h), while those of the control group did not (Fig. S2). These results suggest an accelerated metamorphosis at a higher temperature. Under farm conditions (15 ± 1.14 °C), the hepatosomatic index of *A. davidianus* larvae did not vary with development during 172–342 d.a.h (Fig. S3). Warm-acclimated larvae had drastically enlarged livers, and this phenomenon was repeatedly observed in two independent treatments (Fig. 3a).

Combined transcriptomics and metabolomics were conducted to study the molecular responses to warming. At the transcriptional level, the limb and liver had the greatest and smallest numbers of DEGs, respectively (Fig. 3b). Most of the DEGs showed downregulation at 25 °C in most organs, which was suggestive of thermal acclimation. At the metabolic level, the heart and limb had more differently expressed metabolites (DEMs) than other organs (Fig. 3b). The majority of the DEGs and DEMs were organ-specific (Fig. S4), suggesting prominent organ heterogeneity in thermal responses.

3.3. Metabolic limitations at higher temperatures

There were 199 DEGs (at a threshold of $p < 0.05$) shared by more than four organs. They highlighted the transcriptional regulation of protein translation and processing processes under heat stress, including spliceosome, propanoate metabolism, ribosome, RNA transport, and protein processing in endoplasmic reticulum (Fig. S5-a). Functional enrichment analyses were also conducted for the DEGs of each organ. Protein translation and processing (i.e., spliceosome, protein processing in

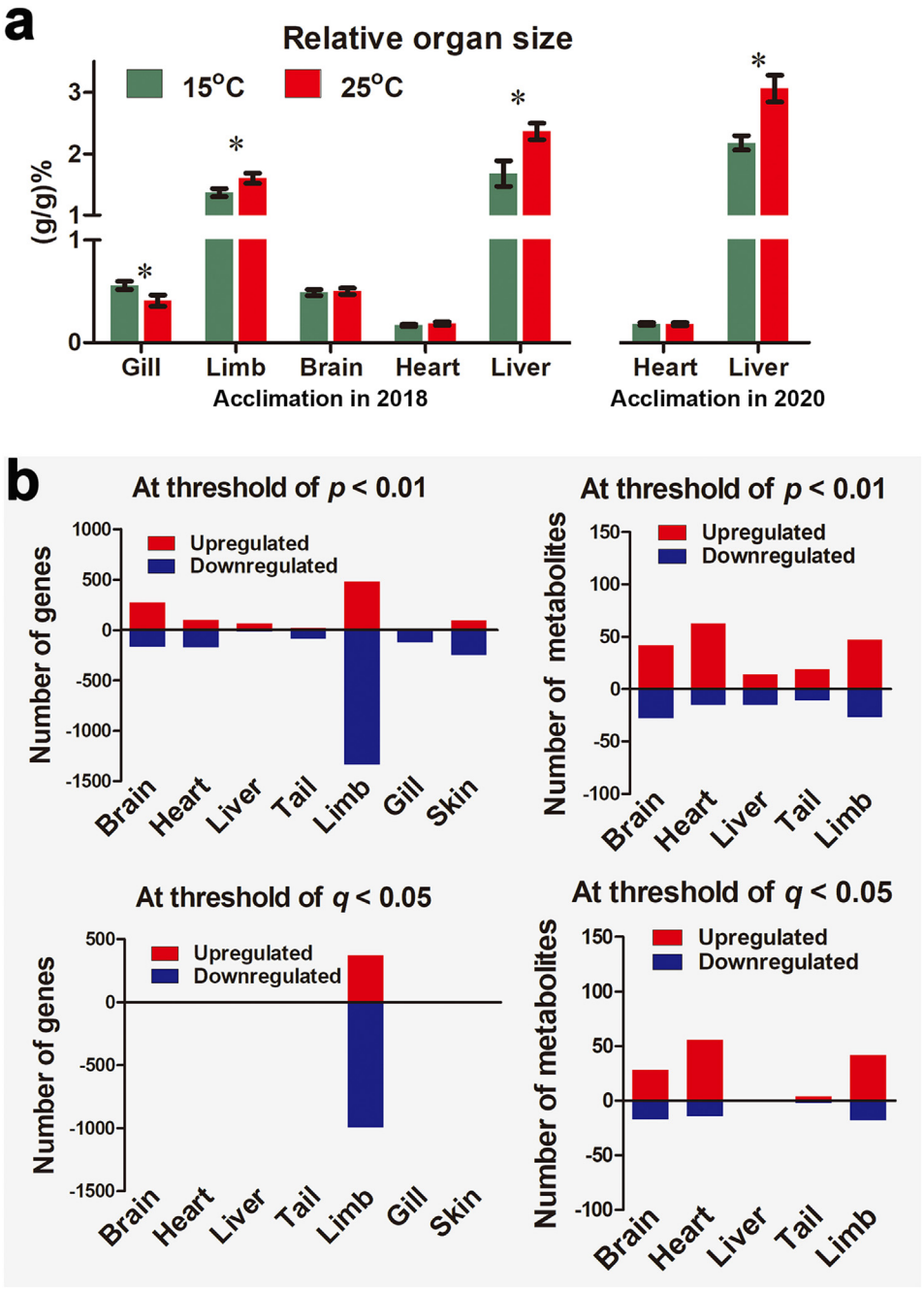

Fig. 3. Organ heterogeneity in thermal responses. (a) Variations in relative organ size at higher temperature. The asterisks denote significant intergroup difference ($p < 0.05$, ANCOVA). (b) Influences of warming on the gene expression and metabolic profiles of *A. davidianus* larvae (warm-acclimated group vs. control). Note the prominent organ heterogeneity in the thermal responses.

endoplasmic reticulum, and ribosome) and oxidative phosphorylation were enriched by upregulated DEGs in multiple organs even at a higher temperature (Fig. 4a). Despite the transcriptional upregulation, we observed decreased protein levels in the livers of the warm-acclimated group (Fig. 4b). These results suggest that the protein synthesis was likely constrained in the warm-acclimated larvae, at least in the liver.

There were 50 DEMs (at a threshold of $p < 0.05$) shared by more than three organs. Warm-acclimated larvae had increased *N*-acetyl-L-tyrosine, acetylcholine, 3alpha-mannobiose, and lysyl-cysteine in all five organs (Fig. S5-b). The shared DEMs highlighted variations in glycerophospholipid metabolism and amino acid metabolism (Fig. S4). To reveal the metabolic pathways that differed between the groups most significantly, the DEMs meeting foldchange >4 were screened out for each organ (Fig. 5a). The nucleotide metabolism was highlighted (Fig. 5b). The purines, pyridines, and nucleoside levels showed overall upregulation in warm-acclimated larvae. The brain, heart, and liver showed additional changes in the levels of nucleoside phosphates. Specifically, most identified nucleoside phosphates decreased in the brain; all the identified nucleoside monophosphates (i.e., AMP, GMP, and UMP) increased in the heart; most identified nucleoside diphosphates and triphosphates (e.g., ADP and GDP) decreased in the liver, while the AMP level increased (Fig. 5c). This variation pattern is a sign of energy deficiency (Hardie et al., 2016).

The TCA cycle and its upstream glycolysis and beta oxidation are critical pathways in energy metabolism. The liver, heart, and brain of warm-acclimated larvae had decreased level of TCA cycle intermediates, and the liver showed an additional reduction in glycolytic metabolites

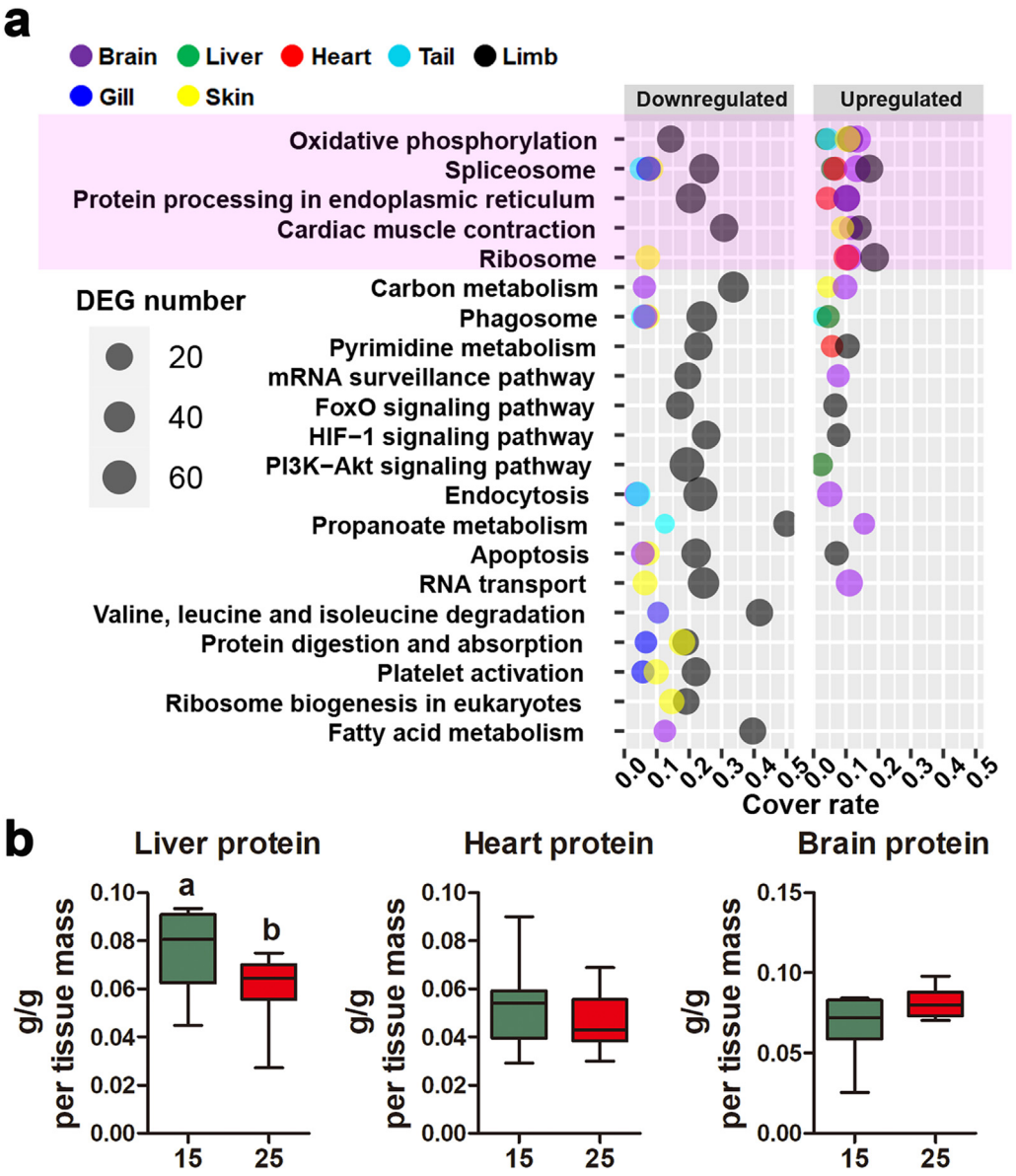

Fig. 4. Warming affected protein metabolism of *A. davidianus* larvae. (a) Metabolic pathways enriched ($p < 0.005$, KOBAS 3.0) by downregulated or upregulated DEGs in warm-acclimated larvae. The cover rate is calculated as the ratio of the numbers of enriched genes to the total number of genes in a given pathway. The color and size of the dots denote the organs and enriched gene numbers, respectively. Only the pathways enriched in at least two organs are presented. The pink background highlights the metabolic pathways enriched by upregulated DEGs in more than three organs. They are mainly the processes involved in protein synthesis (i.e., spliceosome, protein processing in endoplasmic reticulum, and ribosome) and energy metabolism (i.e., oxidative phosphorylation). Note that the enrichment of cardiac muscle contraction was mainly attributed to the DEGs of oxidative phosphorylation. (b) Organ protein levels on the 80th day after acclimation. Different letters denote significant differences between groups at $p < 0.05$ (Mann–Whitney *U* test).

(i.e., fructose 1,6-biphosphate and glyceraldehyde) and beta oxidation metabolites (i.e., stearoyl-carnitine and palmitoyl-carnitine) (Fig. 5d). This was not a result of the proactive transcriptional downregulation of these pathways (Fig. S6). Interestingly, warm-acclimated larvae had increased glycogen levels in their livers (Fig. 5e), in contrast to the variations in glycolytic intermediates. This suggested that the metabolic flux throughout glycolysis was suppressed in larvae from the warm group (Fig. 5f). Meanwhile, the triglyceride (TAG) levels in the blood and liver were unchanged (Fig. 5e). The larvae from the warm group had increased levels of carnitine and acetyl-carnitine in multiple organs (Figs. S5-b and 6), which was suggestive of increased lipid catabolism (Houten et al., 2020). Additionally, the organs of the warm group had decreased aspartate but increased arginosuccinate, which are the substrate and product, respectively, of a critical step in urea cycle (Fig. S5-b). This was accompanied by increased organic acids from amino acid catabolism (e.g., 2-methyl-3-hydroxybutyric acid and methyl-acetoacetic acid) (Fig. S5-b). This suggests an increase in the amino acid catabolism at a higher temperature (Fig. 6).

4. Discussion

4.1. Plastic relationship between temperature and body size in A. davidianus

Global warming likely threatens the survival of wild *A. davidianus* (Zhao et al., 2020). Although these animals may avoid adverse heat waves via behavioral thermoregulation, the increased exposure to sub-optimum temperatures can still have numerous chronic effects on their life traits and population dynamics. Reduced body size in the adult stage is the one of the most well-known outcomes of warming in ectotherms within non-extreme temperature ranges (van Rijn et al., 2017), due to their being more temperature dependent than their growth (Forster et al., 2011).

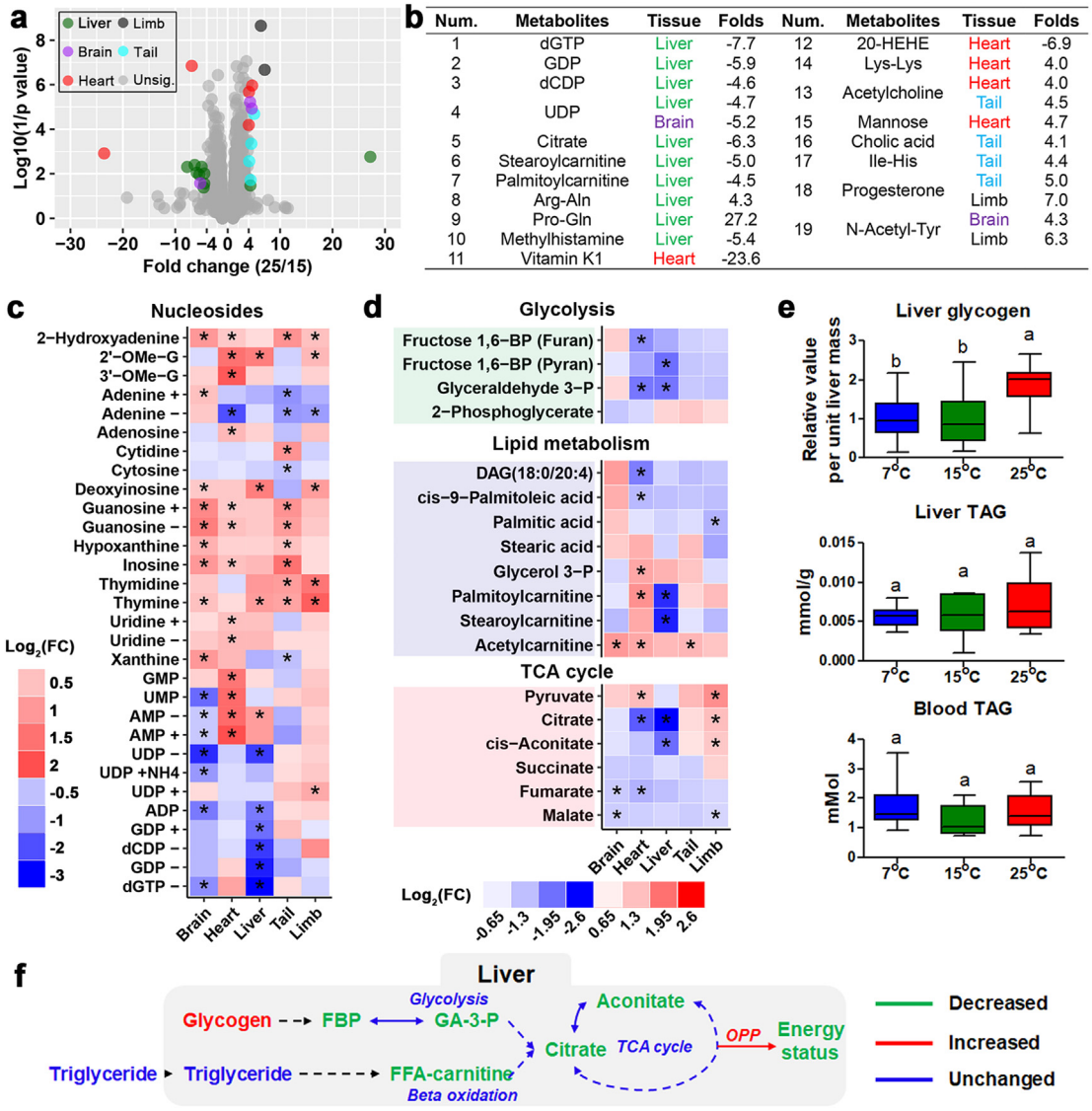

Num.	Metabolites	Tissue	Folds	Num.	Metabolites	Tissue	Folds
1	dGTP	Liver	-7.7	12	20-HEHE	Heart	-6.9
2	GDP	Liver	-5.9	14	Lys-Lys	Heart	4.0
3	dCDP	Liver	-4.6	13	Acetylcholine	Heart	4.0
4	UDP	Liver	-4.7			Tail	4.5
		Brain	-5.2	15	Mannose	Heart	4.7
5	Citrate	Liver	-6.3	16	Cholic acid	Tail	4.1
6	Stearoylcarnitine	Liver	-5.0	17	Ile-His	Tail	4.4
7	Palmitoylcarnitine	Liver	-4.5	18	Progesterone	Tail	5.0
8	Arg-Aln	Liver	4.3			Limb	7.0
9	Pro-Gln	Liver	27.2	19	N-Acetyl-Tyr	Brain	4.3
10	Methylhistamine	Liver	-5.4			Limb	6.3
11	Vitamin K1	Heart	-23.6				

Fig. 5. Warming-affected energy metabolism of *A. davidianus* larvae. (a) Volcano plot presenting the variations in the metabolome of *A. davidianus* larvae. Metabolites that vary drastically (fold change >4 and $p < 0.05$) are colored according to their organs, while the others are in gray. (b) Detailed information on the metabolites varied drastically at a higher temperature. (c–d) The variation pattern of nucleoside derivates (c) and metabolites related to energy metabolism (d). The color of the tiles denotes the fold change, and a darker red or blue color means a larger fold change between groups. The asterisks denote significant differences at $p < 0.05$. (e) Variations in glycogen and TAG levels. Different letters denote significant differences ($p < 0.05$, Kruskal–Wallis test) between groups. (f) Metabolic map presenting the variations in energy metabolism in the liver. The colors of items denote the variation trends, and the text in italics denotes variations at the transcriptional level.

Warm-acclimated *A. davidianus* exhibited accelerated metamorphosis in the form of earlier gill absorption (Figs. 3a and S2). Moreover, we observed increased progesterone levels in the warm group on the 80th day after acclimation (Figs. 3d and 5b). Progesterone is the metabolic intermediate in sex hormone synthesis, and it plays important roles in gametogenesis in both females and males of all vertebrates (Chishti et al., 2013; Hanocq et al., 1974; Miura et al., 2006). Increased progesterone level is a sign of accelerated sexual maturation in larvae at higher temperatures. In addition, the warm-acclimated larvae showed little increase in their growth rate when they were fed red worm. Thus, as was predicted by the TSR, we should expect a dramatic reduction in the body size of adult *A. davidianus* if their primary prey is red worm. However, our results indicated that a fish diet rich in lipid could improve the growth performance at 25 °C effectively (Fig. 2b). Although warming would still cause adult *A. davidianus* to be smaller, the degree of body size reduction would be less dramatic. These results suggest that the relationship between temperature and the body size of *A. davidianus* can be flexible, which is an important discovery in the context of the TSR. In practice, however, it should be noted that the prey rich in lipids may also be susceptible to warming, which may constitute a potential limitation in terms of the thermal adaptation of *A. davidianus*.

4.2. Biological constraints of the growth performance at higher temperatures

On the whole-organism level, warm-acclimated larvae had a reduced food conversion rate. This could be partly explained by the need for increased resource investment into metabolic maintenance (e.g., increased energy consumption for maintaining iron homeostasis and accelerated protein turnover) at a higher temperature (Gillooly et al., 2001). It should be pointed out that the food conversion rate decreased with development (Fig. 1f), and this could potentially contribute to the lower food conversion rate of warm-acclimated larvae due to their higher developmental rate. The decreased food conversion rate with development can also be explained by the diversion of resources from somatic growth to other physiological functions (e.g., sexual maturity and reproduction). The reduced food conversion rate is likely the result of both the direct and indirect effects of warming from the perspective of resource allocation. Although a reduction in

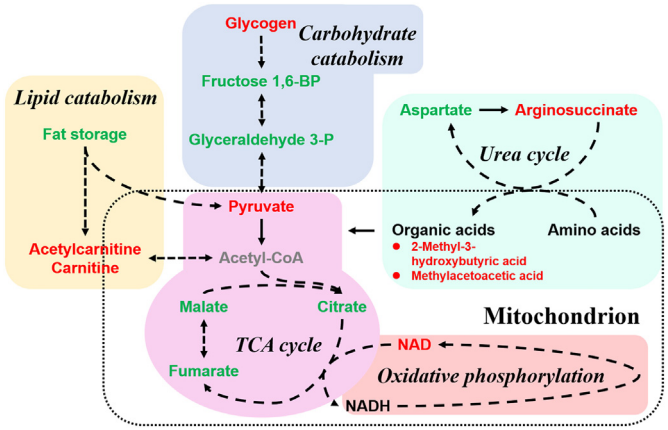

Fig. 6. An integrated metabolic map explaining the metabolic changes in larvae at a higher temperature. The color of a metabolite denotes the variation trends at a higher temperature: red, increased; green, decreased. Solid arrow, one-step reaction; dashed arrow, multi-step reaction. The variation patterns of these metabolites suggest disorder in the glycol-metabolism of the warming group, and the lipids and amino acids are mobilized to support the tight energy budget.

resource allocation to growth has been considered a major cause for reduced body size at higher temperatures if food is limited (Sheridan and Bickford, 2011), it might not fully explain our observations as sufficient food was provided. This means that some additional factors likely constrained the growth performance of warm-acclimated *A. davidianus* larvae.

At the organ level, warm-acclimated larvae had reduced relative tail lengths and enlarged livers. It should be noted that the relative tail length of *A. davidianus* larvae decreases with development (Fig. 1g–h). Thus, their accelerated development may be a reason for the shorter tail of the warm-acclimated larvae. The relative tail length of the individuals who developed at 25 °C after only 55 days was shorter than those of their counterparts who developed at 15 °C after 95 days (Fig. 1g–h; the statistical results are not presented). Thus, it is possible that direct heat stress may also contribute to the reduced tail length at a higher temperature. The tail is not only a major locomotive organ but also the primary fat depot of *A. davidianus* (Li et al., 2010; Li et al., 1992). Accordingly, a shorter tail potentially means reduced fat storage. This is consistent with the increased lipid catabolism at 25 °C (Fig. 6). Such a morphological change likely impacts the locomotive capacity of *A. davidianus* and reduces their tolerance to starvation during non-feeding seasons (e.g., winter). Given that the relative liver size of *A. davidianus* did not vary with development 172–342 d.a.h (Fig. S3), the large liver observed in warm-acclimated larvae is likely the result of thermal effects. The liver enlargement of warm-acclimated larvae was accompanied by increased hepatic glycogen levels (Fig. 4b). Interestingly, this phenomenon resembles the symptoms of glycogen storage disease (GSD) in mammals. GSD is typically caused by a deficiency of the enzymes involved in glycogen metabolism, resulting in the accumulation of hepatic glycogen and the enlargement of the liver (Ozen, 2007). As the endogenous glucose production is suppressed, the falling insulin levels permit the catabolism of tissue protein and fat storage in GSD (Roach, 2002). This is exactly what we observed in the warm-acclimated *A. davidianus* larvae. In contrast to glycogen accumulation, we observed a severe decrease in the intermediates of energy metabolism in the liver. For example, the acylcarnitines decreased in the liver but remained unchanged or even increased in other organs (Fig. 5d). This means that the liver likely suffered from having a tight energy budget. The liver is responsible for the synthesis of a large amount of protein, including albumin, the most abundant protein in blood serum. Given that protein synthesis accounts for the largest proportion of the cellular energy budget (Hochachka et al., 1996), it is not surprising that the protein level decreased in the liver of warm-acclimated larvae. These results suggested that the liver was likely more sensitive to warming than other organs in *A. davidianus* larvae. Considering the central role of the liver in vertebrate metabolism, a metabolic problem that affects it directly might constitute a limitation for the somatic growth of *A. davidianus* larvae.

Since the differences in developmental stages between thermal groups can also cause prominent molecular changes, the mere quantitative variations in gene expression or metabolite levels cannot be considered the outcome of direct thermal stress, unless the changes show clear signs of metabolic disorder or they contradict other changes. At the molecular level, protein synthesis and energy production were transcriptionally upregulated in multiple organs even at higher temperature (Fig. 4). This implies that the activity of these two processes most likely constrained the overall metabolic intensity at a higher temperature from the perspective of homeostasis. This speculation is supported by the decreased hepatic protein level (Fig. 4b) and increased nucleoside monophosphate levels (Fig. 5c), which are signs of energy deficiency (Hardie et al., 2016). As protein synthesis and energy production have central roles in determining cell growth (Dai and Zhu, 2020; Hietakangas and Cohen, 2009), their activity could directly cause the poor growth performance of worm-fed larvae at a higher temperature. Furthermore, the energy status of warm-acclimated larvae was likely constrained by the metabolic flux throughout the upstream catabolic processes, as these larvae had decreased glycolytic and TCA cycle intermediates and increased NAD, which is a critical substrate of catabolism (Fig. 6). Most importantly, the inverse variation trend between glycolytic metabolites and glycogen levels indicates deficient glycogen metabolism in the warm-acclimated larvae (Fig. 5f). This is consistent with the increased lipid and amino acid metabolism at a higher temperature (Fig. 6). Such a metabolic switch likely tightened the trade-off in resource allocation between biosynthesis and maintenance, and explains the energy status, shortened tail (fat depot), and poor growth performance in warm-acclimated larvae (Fig. 7a). Moreover, the deficient glycogen metabolism may explain the different outcomes in terms of the growth rate

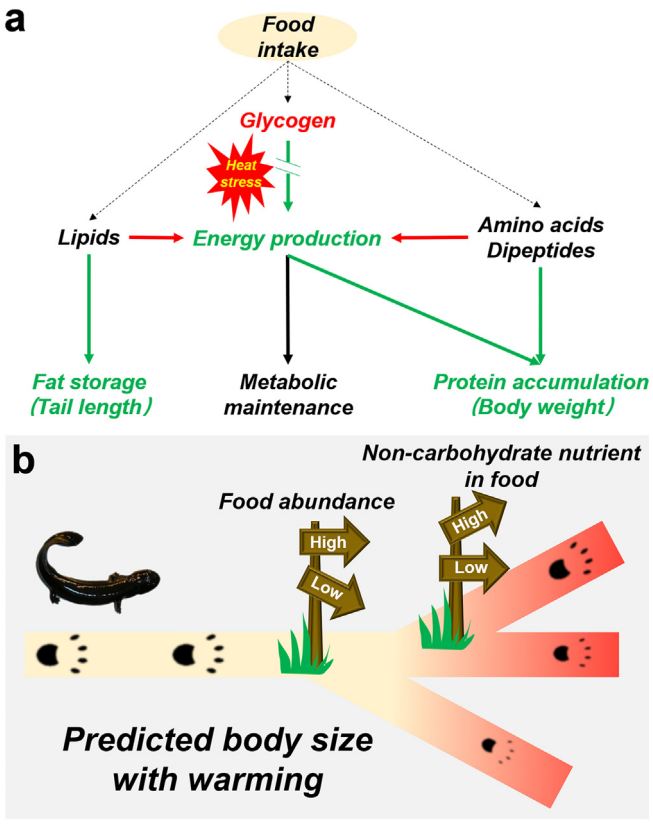

Fig. 7. Summary on the influences of warming on the body size of *A. davidianus* larvae. (a) Deduced mechanism underlying the poor growth performance of worm-fed larvae at a higher temperature. Red color, increased or upregulated; green color, deceased or downregulated. (b) Nutrient dependence of body size reduction with warming.

between fish and worm diets, even when both were provided sufficiently. The worm diet contains much more carbohydrate, which, once converted to glycogen, cannot be efficiently mobilized at a higher temperature. It means that the larvae needs to consume more worms than fish diet to reach the same cellular energy status at a higher temperature. However, increasing the consumption of worms may not be possible for larvae as it likely aggravates the hepatic glycogen accumulation and affects its physiological functions (Burda and Hochuli, 2015). Taken together, our results suggest that warming likely impacts the glycogen metabolism of *A. davidianus* larvae, and the resulting metabolic shift to lipids and amino acids constrained their body growth at a higher temperature (Fig. 7a).

4.3. Conservation implications in the context of global warming

Although the TSR suggest that ectotherms' body size will be reduced as a result of rising of temperatures, it does not account for the flexibility of the relationship between body size and temperature. In this study, *A. davidianus* larvae at higher temperature exhibit decreased food conversion rate and deficiency in glycogen metabolism. This means that both the food abundance and nutrient composition can shape the variation in body size with temperature (Fig. 7b). Further studies should focus on the influence of warming on the food/prey preferences (with different nutrient compositions) of *A. davidianus* to assess whether these animals can undergo behavior regulation to improve their metabolic and physiological performance in warmer conditions. From a conservation perspective, increasing the prey diversity in their habitats would be beneficial to *A. davidianus*, and this approach may be applied in practice, e.g., translocation and reintroduction. Furthermore, prey abundance and diversity in their wild habitats should be taken into consideration when assessing the population dynamics of *A. davidianus* in the future.

Further molecular studies are required to identify the enzymes that constrains its glycogen metabolism at higher temperatures. Since *A. davidianus* has been classified into several genetic clades (Yan et al., 2018), it would be interesting to study whether there were differences in the growth performance and glycogen metabolic capacity between clades. This knowledge would be useful for evolutionary and conservation biology.

5. Conclusion

In this study, we compared the growth performance of *A. davidianus* larvae at two typical temperatures (15 °C, empirical optimum; 25 °C, suboptimal and near the highest temperature in their wild habitats) to investigate how warming will affect the body size of the largest extant amphibian. We found that the relationship between the temperature and the growth rate varied with the food type. When larvae were fed red worms, the increase in the growth rate at a higher temperature was limited. In combination with accelerated development, we might expect to see a drastic reduction in the body size of adult *A. davidianus*. However, when fed fish fry, which is rich in lipid and had less carbohydrate, the growth performance of *A. davidianus* improved greatly at a higher temperature, implying a samller reduction in body size. This suggests that the relationship between temperature and body size may be flexible in this species, which is an important discovery in the context of the TSR. The underlying mechanisms were revealed. Our results suggest that warming causes symptoms resembling glycogen storage disease (e.g., enlarged liver) in *A. davidianus* larvae. The defects in glycogen metabolism limited the metabolic flux throughout glycolysis, and this was accompanied by increased mobilization of lipids and amino acids to support energy metabolism. Such a metabolic switch tightens the trade-off in resource allocation and thus limits somatic growth at higher temperatures. Additionally, glycogen accumulation in the liver prevents the excessive consumption of a diet rich in carbohydrate, which may explain the different outcomes of individuals fed a worm or fish diet, though both were provided sufficiently. These results indicate that both the food abundance and nutrient composition can influence the variation in body size with warming in *A. davidianus*. These findings could have great significance for the conservation of this important amphibian.

Supplementary data to this article can be found online at https://doi.org/10.1016/j.scitotenv.2022.160105.

Funding

This work was supported by the National Key Research and Development Program of China (2016YFC0503200), Biodiversity Survey and Assessment Project of the Ministry of Ecology and Environment, China (2019HJ2096001006), Construction of Basic Conditions Platform of Sichuan Science and Technology Department (2019JDPT0020), and China Biodiversity Observation Networks (Sino BON).

Ethics

All animal protocols in this study were reviewed and approved by the Animal Ethical and Welfare Committee of Chengdu Institute of Biology, Chinese Academy of Sciences (permit: CIB20160305 and 20191105), in compliance with the ARRIVE guidelines 2.0 (Percie du Sert et al., 2020) and Guide for the Care and Use of Laboratory Animals (8th edition) published by National Research Council (US) Committee for the Update of the Guide for the Care and Use of Laboratory Animals (2011).

CRediT authorship contribution statement

Conceptualization, W.Z. and J-P.J.; methodology, C-L.Z., W.Z., and T.Z.; formal analysis, W.Z. and J-Y.L.; investigation, W.Z., C-L.Z., and T.Z.; resources, C-L.Z. T.Z., J-P.J., C.L. and F.X.; writing-original draft preparation, W.Z.; writing-review and editing, W.Z.; visualization, W.Z.; supervision, W.Z., T.Z., and J-P.J.; project administration, J-P.J.; funding acquisition, J-P.J. All authors have read and agreed to the published version of the manuscript.

Data availability

The data used for the analyses presented here are available from supplementary data. Sequencing data have been uploaded to https://ngdc.cncb.ac.cn/gsa/, with the accession number CRA006550.

Declaration of competing interest

The authors declare that they have no known competing financial interests or personal relationships that could have appeared to influence the work reported in this paper.

Acknowledgments

The authors thank for the Cheng-Xin Hu, Yan Wang, and Wen-Bo Zhu for help in sample collection and animal daily care.

References

Atkinson, D., 1994. Temperature and organism size-a biological law for ectotherms? Adv. Ecol. Res. 25, 1–58.

Atkinson, D., Morley, S.A., Hughes, R.N., 2006. From cells to colonies: at what levels of body organization does the 'temperature-size rule' apply? Evol.Dev. 8, 202–214.

Baudron, A.R., Needle, C.L., Rijnsdorp, A.D., Tara, Marshall C., 2014. Warming temperatures and smaller body sizes: synchronous changes in growth of North Sea fishes. Glob. Chang. Biol. 20, 1023–1031.

Bizer, J.R., 1978. Growth rates and size at metamorphosis of high elevation populations of *Ambystoma tigrinum*. Oecologia 34, 175–184.

Brose, U., Dunne, J.A., Montoya, J.M., Petchey, O.L., Schneider, F.D., Jacob, U., 2012. Climate change in size-structured ecosystems. Philos. Trans. R. Soc. Lond. Ser. B Biol. Sci. 367, 2903–2912.

Burda, P., Hochuli, M., 2015. Hepatic glycogen storage disorders: what have we learned in recent years? Curr.Opin.Clin.Nutr.Metab.Care 18 (4), 415–421.

Chen, X.B., Shen, J.Z., Zhao, J.Y., Xiong, J.J., Zhang, G.L., 1999. The effect of water temperature on intake of *Andrias davidianus* (in Chinese). Fish. Sci. 1, 20–22.

Chishti, Y.Z., Feswick, A., Munkittrick, K.R., Martyniuk, C.J., 2013. Transcriptomic profiling of progesterone in the male fathead minnow (*Pimephales promelas*) testis. Gen. Comp. Endocrinol. 192, 115–125.

Claësson, D., Wang, T., Malte, H., 2016. Maximal oxygen consumption increases with temperature in the European eel (*Anguilla anguilla*) through increased heart rate and arteriovenous extraction. Conserv. Physiol. 4 (1), cow027.
Dai, X.-F., Zhu, M.-L., 2020. Coupling of ribosome synthesis and translational capacity with cell growth. Trends Biochem. Sci. 45, 681–692.
Daufresne, M., Lengfellner, K., Sommer, U., 2009. Global warming benefits the small in aquatic ecosystems. Proc. Natl. Acad. Sci. U. S. A. 106, 12788–12793.
Davidowitz, G., Nijhout, H.F., 2004. The physiological basis of reaction norms: the interaction among growth rate, the duration of growth and body size1. Integr. Comp. Biol. 44, 443–449.
DeLong, J.P., Gilbert, B., Shurin, J.B., Savage, V.M., Barton, B.T., Clements, C.F., et al., 2015. The body size dependence of trophic cascades. Am. Nat. 185, 354–366.
Eliason Erika, J., Clark Timothy, D., Hague Merran, J., Hanson Linda, M., Gallagher Zoë, S., Jeffries Ken, M., et al., 2011. Differences in thermal tolerance among sockeye salmon populations. Science 332, 109–112.
Fan, W.-B., Zhu, W.-B., Zhang, M.-H., Zhao, T., Jiang, J.-P., 2022. Preliminary studies on the early development of *Andrias davidianus*. Sichuan J.Zool. 41, 517–525.
Fei, L., Hu, S.-Q., Ye, C.-Y., Huang, Y.-Z., et al., 2006. Fauna Sinica, Amphibia Vol. 1, Amphibia Gymnophiona and Urodela. Science Press, Beijing.
Fischer, K., Fiedler, K., 2002. Reaction norms for age and size at maturity in response to temperature: a test of the compound interest hypothesis. Evol. Ecol. 16, 333–349.
Forster, J., Hirst, A.G., Woodward, G., 2011. Growth and development rates have different thermal responses. Am. Nat. 178, 668–678.
Forster, J., Hirst, A.G., Atkinson, D., 2012. Warming-induced reductions in body size are greater in aquatic than terrestrial species. Proc. Natl. Acad. Sci. 109, 19310–19314.
Fryxell, D.C., Hoover, A.N., Alvarez, D.A., Arnesen, F.J., Benavente, J.N., Moffett, E.R., et al., 2020. Recent warming reduces the reproductive advantage of large size and contributes to evolutionary downsizing in nature. Proc. R. Soc. B Biol. Sci. 287, 20200608.
Gao, K.Q., Shubin, N.H., 2003. Earliest known crown-group salamanders. Nature 422, 424–428.
Gardner, J.L., Peters, A., Kearney, M.R., Joseph, L., Heinsohn, R., 2011. Declining body size: a third universal response to warming? Trends Ecol. Evol. 26, 285–291.
Ge, Y.-R., Zheng, H.-X., 1994. Natural breeding cycle of the giant salamander (*Andrias davidianus*). J.Henan Hormal Univ.(Nat.Sci.) 22, 67–70.
Ghosh, S.M., Testa, N.D., Shingleton, A.W., 2013. Temperature-size rule is mediated by thermal plasticity of critical size in *Drosophila melanogaster*. Proc. R. Soc. B Biol. Sci. 280 (1760), 20130174.
Gillooly, J.F., Brown, J.H., West, G.B., Savage, V.M., Charnov, E.L., 2001. Effects of size and temperature on metabolic rate. Science 293, 2248–2251.
Grans, A., Jutfelt, F., Sandblom, E., Jonsson, E., Wiklander, K., Seth, H., et al., 2014. Aerobic scope fails to explain the detrimental effects on growth resulting from warming and elevated CO2 in Atlantic halibut. J. Exp. Biol. 217, 711–717.
Gunderson, A.R., Stillman, J.H., 2015. Plasticity in thermal tolerance has limited potential to buffer ectotherms from global warming. Proc. Biol.Sci. 282, 20150401.
Hanocq, F., De Schutter, A., Hubert, E., Brachet, J., 1974. Cytochemical and biochemical studies on progesterone-induced maturation in amphibian oocytes: 2.DNA synthesis. Differentiation 2, 75–90.
Hardie, D.G., Schaffer, B.E., Brunet, A., 2016. AMPK: an energy-sensing pathway with multiple inputs and outputs. Trends Cell Biol. 26, 190–201.
Heatwole, H., Torres, F., Blasini De Austin, S., Heatwole, A., 1969. Studies on anuran water balance—I. Dynamics of evaporative water loss by the coquí, *eleutherodactylus portoricensis*. Comp. Biochem. Physiol. 28 (1), 245–269.
Heino, M., Kaitala, V., 2001. Evolution of resource allocation between growth and reproduction in animals with indeterminate growth. J. Evol. Biol. 12, 423–429.
Hietakangas, V., Cohen, S.M., 2009. Regulation of tissue growth through nutrient sensing. Annu. Rev. Genet. 43, 389–410.
Hochachka, P.W., Buck, L.T., Doll, C.J., Land, S.C., 1996. Unifying theory of hypoxia tolerance: molecular/metabolic defense and rescue mechanisms for surviving oxygen lack. Proc. Natl. Acad. Sci. 93, 9493.
Houten, S.M., Wanders, R.J.A., Ranea-Robles, P., 2020. Metabolic interactions between peroxisomes and mitochondria with a special focus on acylcarnitine metabolism. Biochim. Biophys. Acta Mol. basis Dis. 1866, 165720.
Hu, Q.M., Tian, H.F., Xiao, H.B., 2019. Effects of temperature and sex steroids on sex ratio, growth, and growth-related gene expression in the Chinese giant salamander *Andrias davidianus*. Aquat. Biol. 28, 79–90.
Hughes, L., 2000. Biological consequences of global warming: is the signal already apparent? Trends Ecol. Evol. 15, 56–61.
IPCC, 2021. AR6 Climate Change 2021: The Physical Science Basis.
IUCN, 2016. IUCN Red List of Threatened Species. http://www.iucnredlist.org/initiatives/amphibians.
Jiang, J.-P., Xie, F., Zang, C.-X., Cai, L., Li, C., Wang, B., et al., 2016. Assessing the threat status of amphibians in China. Biodivers. Sci. 24, 588–597.
Jiang, J.-P., Xie, F., Li, C., Wang, B., 2021. China's Red List of Biodiversity: Vertebrates. AmphibiansVol. IV. Science Press, Beijing.
Johansen, J.L., Pratchett, M.S., Messmer, V., Coker, D.J., Tobin, A.J., Hoey, A.S., 2015. Large predatory coral trout species unlikely to meet increasing energetic demands in a warming ocean. Sci. Rep. 5, 13830.
Jurasinski, G., Retzer, V., 2012. simba: a collection of functions for similarity analysis of vegetation data. R package version 0.3-5. Available online at: https://cran.r-project.org/web/packages/simba/index.html.
Kearney, M., Shine, R., Porter, W.P., 2009. The potential for behavioral thermoregulation to buffer "cold-blooded" animals against climate warming. Proc. Natl. Acad. Sci. 106, 3835–3840.
Kuparinen, A., Cano, J.M., Loehr, J., Herczeg, G., Gonda, A., Merilä, J., 2011. Fish age at maturation is influenced by temperature independently of growth. Oecologia 167, 435–443.
Lefevre, S., 2016. Are global warming and ocean acidification conspiring against marine ectotherms? A meta-analysis of the respiratory effects of elevated temperature, high CO2 and their interaction. Conserv. Physiol. 4, cow009.
Lemieux, H., Tardif, J.-C., Dutil, J.-D., Blier, P.U., 2010. Thermal sensitivity of cardiac mitochondrial metabolism in an ectothermic species from a cold environment, Atlantic wolffish (*Anarhichas lupus*). J. Exp. Mar. Biol. Ecol. 384, 113–118.
Li, P.-P., Zhang, Y.-H., Fang, R.-S., 1992. On fat organs of *Andrias davidianus* and comparison with *Batrachuperus pinchonii* and *Cynopus orientalis*. J. Shanxi Norm. Univ. (Nat.Sci.Ed.) 20, 59–79.
Li, L.-Q., Zan, L.-S., Tian, W.-Q., Li, Z.-C., Meng, M., 2010. Adipose tissue distribution and physical and chemical properties of *Andrias davidianus*. Acta Agric.Boreali-occdentalis Sin. 19, 7–10.
Miura, T., Higuchi, M., Ozaki, Y., Ohta, T., Miura, C., 2006. Progestin is an essential factor for the initiation of the meiosis in spermatogenetic cells of the eel. Proc. Natl. Acad. Sci. U. S. A. 103, 7333–7338.
Mu, H.-M., Li, Y., Yao, J.-K., Ma, S., 2011. A review: current research on biology of Chinese giant salamander. Fish. Sci. 30, 513–516.
National Research Council (US) Committee for the Update of the Guide for the Care and Use of Laboratory Animals, 2011. Guide for the Care and Use of Laboratory Animals. 8th edition. National Academies Press (US), Washington (DC).
Ohlberger, J., 2013. Climate warming and ectotherm body size – from individual physiology to community ecology. Funct. Ecol. 27, 991–1001.
Ortega, Z., Mencía, A., Pérez-Mellado, V., 2016. Behavioral buffering of global warming in a cold-adapted lizard. Ecol.Evol. 6, 4582–4590.
Ozen, H., 2007. Glycogen storage diseases: new perspectives. World J. Gastroenterol. 13, 2541–2553.
Peig, J., Green, A.J., 2009. New perspectives for estimating body condition from mass/length data: the scaled mass index as an alternative method. Oikos 118, 1883–1891.
Percie du Sert, N., Ahluwalia, A., Alam, S., Avey, M.T., Baker, M., Browne, W.J., et al., 2020. Reporting animal research: explanation and elaboration for the ARRIVE guidelines 2.0. PLoS Biol. 18, e3000411.
Pörtner, H.O., 2002. Climate variations and the physiological basis of temperature dependent biogeography: systemic to molecular hierarchy of thermal tolerance in animals. Comp. Biochem. Physiol. A Mol. Integr. Physiol. 132, 739–761.
Pörtner, H.O., Farrell, A.P., 2008. Physiology and climate change. Science 322 (5902), 690–692.
Roach, P., 2002. Glycogen and its metabolism. Curr. Mol. Med. 2, 101–120.
Rudolf, V.H., 2012. Seasonal shifts in predator body size diversity and trophic interactions in size-structured predator-prey systems. J. Anim. Ecol. 81, 524–532.
Sheridan, J.A., Bickford, D., 2011. Shrinking body size as an ecological response to climate change. Nat. Clim. Chang. 1, 401–406.
van Rijn, I., Buba, Y., DeLong, J., Kiflawi, M., Belmaker, J., 2017. Large but uneven reduction in fish size across species in relation to changing sea temperatures. Glob. Chang. Biol. 23, 3667–3674.
Wang, H.-W., 2004. The artificial culture of Chinese giant salamander. J. Aquac. 25, 41–44.
Wang, W.L., Du, X.Q., Zhang, L.Q., Shan, G.F., 2002. Investigation on the breeding biology of giant salamanders (*Andrias davidianus*). J. Henan Educ. Inst. (Nat. Sci.) 11, 21–22.
Wang, J., Zhang, H., Xie, F., Wei, G., Jiang, J.-P., 2017. Genetic bottlenecks of the wild Chinese giant salamander in karst caves. Asian Herpetol.Res. 8, 174–183.
Warton, D.I., Duursma, R.A., Falster, D.S., Taskinen, S., 2012. Smatr 3– an R package for estimation and inference about allometric lines. Methods Ecol. Evol. 3, 257–259.
Wickham, H., 2009. Ggplot2: Elegant Graphics for Data Analysis. Springer Publishing Company, Incorporated, New York, NY, USA.
Yan, F., Lü, J., Zhang, B., Yuan, Z., Zhao, H., Huang, S., et al., 2018. The Chinese giant salamander exemplifies the hidden extinction of cryptic species. Curr. Biol. 28, R590–R592.
Ye, Y.-Z., Zhang, H., Li, J., Lai, R., Yang, S., Du, W.-G., 2021. Molecular sensors for temperature detection during behavioral thermoregulation in turtle embryos. Curr. Biol. 31, 2995–3003.e4.
Zhang, L., Kouba, A., Wang, Q.J., Zhao, H., Jiang, W., Willard, S., et al., 2014. The effect of water temperature on the growth of captive Chinese giant salamanders (*Andrias davidianus*) reared for reintroduction: a comparison with wild salamander body condition. Herpetologica 70, 369–377.
Zhang, Z., Mammola, S., Liang, Z., Capinha, C., Wei, Q., Wu, Y., et al., 2020. Future climate change will severely reduce habitat suitability of the critically endangered Chinese giant salamander. Freshw. Biol. 65, 971–980.
Zhao, T., Zhang, W.-Y., Zhou, J., Zhao, C.-L., Liu, X.-K., Liu, Z.-D., et al., 2020. Niche divergence of evolutionarily significant units with implications for repopulation programs of the world's largest amphibians. Sci. Total Environ. 738, 140269.
Zhao, C.-L., Zhao, T., Feng, J.-Y., Chang, L.-M., Zheng, P.-Y., Fu, S.-J., et al., 2022. Temperature and diet acclimation modify the acute thermal performance of the largest extant amphibian. Animals 12, 531.
Zhu, W., Zhang, M.-H., Chang, L.-M., Zhu, W.-B., Li, C., Xie, F., et al., 2019. Characterizing the composition, metabolism and physiological functions of the fatty liver in *Rana omeimontis* tadpoles. Front. Zool. 16, 42.
Zhu, L.-F., Zhu, W., Zhao, T., Chen, H., Zhao, C.-L., Xu, L.-L., et al., 2021a. Environmental temperatures affect the gastrointestinal microbes of the Chinese giant salamander. Front. Microbiol. 12, 543767.
Zhu, W., Chang, L.-M., Shu, G.-C., Wang, B., Jiang, J.-P., 2021b. Fatter or stronger: resource allocation strategy and the underlying metabolic mechanisms in amphibian tadpoles. Comp. Biochem. Physiol. Part D Genomics Proteomics 38, 100825.
Zhu, W., Zhao, C.-L., Feng, J.-Y., Chang, J., Chang, L.-M., Liu, J.-Y., et al., 2022a. Effects of habitat river microbiome on the symbiotic microbiota and multi-organ gene expression of captive-bred Chinese giant salamander. Front. Microbiol. 13, 884880.
Zhu, W., Zhao, C.-L., Zhao, T., Chang, L.-M., Chen, Q.-H., Liu, J.-Y., et al., 2022. Rising floor and dropping ceiling: organ heterogeneity in response to cold acclimation of the largest extant amphibian. Proc. R. Soc. B 20221394.